

PREDICTIONS FOR STATISTICAL PROPERTIES OF FORMING SPHEROIDAL GALAXIES

F. PERROTTA^{1,2}, M. MAGLIOCCHETTI², C. BACCIGALUPI², M. BARTELMANN³, G. DE ZOTTI¹, G.L. GRANATO¹,
L. SILVA⁴, L. DANESE²

¹ OSSERVATORIO ASTRONOMIC DI PADOVA, VICOLO DELL'OSSERVATORIO 5, I-35122 PADOVA, ITALY

² SISSA/ISAS, VIA BEIRUT 4, I-34014 TRIESTE, ITALY

³ MAX-PLANCK INSTITUT FÜR ASTROPHYSIK, P.O. BOX 1317, D-85741 GARCHING, GERMANY

⁴ OSSERVATORIO ASTRONOMIC DI TRIESTE, VIA G. B. Tiepolo, 11, 34131 TRIESTE, ITALY

August 6, 2002

ABSTRACT

We show that the features of the recent astrophysically motivated model by Granato et al. (2001) are fully consistent with the available statistical measurements of galaxies at (sub)-mm wavelengths. We quantitatively predict the impact of this scenario on near future cosmological observations dealing with spatial and flux statistical distribution of (sub)-mm galaxies.

We show that the expected angular correlation function of Spheroids is compatible with available data. We compute the expected power spectrum of fluctuations due to clustering at the frequencies of the High Frequency Instrument (HFI) of ESA's PLANCK satellite: the clustering signal is found to be detectable in regions of low interstellar dust emission.

A further distinctive prediction of the adopted model is a remarkably high fraction of gravitationally lensed sources at bright mm/sub-mm fluxes. In fact, since most Spheroids burn at redshift $z \simeq 2 - 3$ according to the adopted model, gravitational lensing amplifies a significant number of high- z forming spheroidal galaxies which will be detectable by large area, shallow surveys at mm/sub-mm wavelengths, such as those carried out by PLANCK/HFI. Allowing for other source populations, we find that the fraction of gravitationally lensed sources at bright mm/sub-mm fluxes is expected to be up to $\simeq 40\%$.

1. INTRODUCTION

The formation and early evolution of massive spheroidal galaxies is still a most controversial issue (see e.g. Peebles 2002 for a recent review). In the general framework of the hierarchical clustering picture for structure formation in Cold Dark Matter (CDM) cosmologies, two scenarios are confronting each other. According to the “monolithic” scenario, a large fraction of giant elliptical galaxies formed most of their stars in a single gigantic star-burst at high redshift, and then essentially underwent passive evolution. This approach is in contrast with the “merging” scenario, backed up by semi-analytic galaxy formation models (e.g. Kauffmann 1996; Baugh et al. 1998), wherein large galaxies mostly formed via mergers of smaller sub-units that, at the time of merging, had already converted part of their gas into stars. These two scenarios yield very different predictions for the evolution of large ellipticals: if “monolithic” collapse is assumed, the comoving number density of such galaxies remains essentially constant with redshift, while their bolometric luminosity increases with look-back time out to their epoch of formation. On the contrary, according to the “merging” scenario, the comoving density of large ellipticals decreases with increasing redshift.

The evolution of the comoving density in the optical band has however proven difficult to measure, and discordant results have been reported. A deficit of old ellipticals at $z \gtrsim 1$, when compared to predictions from pure luminosity evolution models, has been claimed by several groups (Kauffmann et al. 1996; Zepf 1997; Franceschini et al. 1998; Barger et al. 1999b; Menanteau et al. 1999; Treu & Stiavelli 1999; Rodighiero et al. 2001), while others found evidence for a constant comoving density up to $z \sim 1.5$ (Totani & Yoshii 1997; Benitez al. 1999; Broadhurst & Bowens 2000; Scodreggio & Silva 2000; Cohen 2001). Furthermore, Daddi et al. (2000) find that the observed surface density of Extremely Red Objects (EROs) – the bulk of which

appears to be passively evolving ellipticals – is consistent with predictions from the “monolithic” scenario.

The results of SCUBA and MAMBO surveys at sub-mm/mm wavelengths present a challenge for the current versions of semi-analytical models. The most exhaustive investigation carried out so far (Granato et al. 2000) combines the semi-analytic galaxy formation model by the Durham group (Cole et al. 2000) with the state-of-the-art spectro-photometric code by Silva et al. (1998) which includes reprocessing of starlight by dust. It turns out that, while this approach successfully accounts for a large variety of observables (spectral energy distributions of galaxies of different morphological classes, luminosity functions over a wide wavelength range, from UV to far-IR, and more), it nevertheless falls short by a substantial factor when trying to account for the mm/sub-mm counts. Similarly, Devriendt & Guiderdoni (2000), who used a totally independent semi-analytic model, were forced to introduce an ad-hoc galaxy population to reproduce such counts.

The main problem stems from the fact that, although only a handful of redshifts of SCUBA/MAMBO sources have been reliably measured so far, there is growing circumstantial evidence that many (perhaps most) of them are ultraluminous star-forming galaxies at $z \gtrsim 2$ (Smail et al. 2001; Dunlop 2001a,b; Carilli et al. 2001; Bertoldi et al. 2000; Scott et al. 2001; Fox et al. 2001; Webb et al. 2002b). Furthermore, the inferred star-formation rates are very high (typically from a few hundreds to $\sim 1000 M_{\odot} \text{yr}^{-1}$), consistent with those required to build the stellar populations of massive ellipticals on a timescale $\lesssim 1$ Gyr.

A detailed, astrophysically grounded, model which fully accounts for both the SCUBA/MAMBO counts and for the main aspects of the chemical evolution of spheroidal galaxies (stellar metallicity, luminosity-metallicity relationship, α enhancement), in the framework of the hierarchical clustering scenario, has been recently presented by Granato et al. (2001). Key ingredients of this model are: i) a tight relationship between forma-

tion and early evolution of spheroidal galaxies and active nuclei hosted at their centers (see also Haehnelt & Rees 1993, Silk & Rees 1998, Haehnelt et al. 1998, Cavaliere & Vittorini 1998, Archibald et al. 2001); ii) once the effects of cooling and heating (the latter being mostly due to stellar feedback) are properly taken into account, the timescale for star formation within virialised dark matter (DM) halos turns out to be relatively short for massive spheroidal galaxies while it is longer in the case of less massive halos, where the feedback from supernovae (and/or the active nucleus) slows down the star formation and can also expel a significant fraction of the gas. It therefore follows that the canonical scheme implied by the hierarchical CDM scenario – small clumps collapse first –, while still holding for the dark matter haloes, is reversed for the star formation.

During the active star-formation phase, large spheroidal galaxies show up as luminous sub-mm sources, accounting for the SCUBA and MAMBO counts. The subsequent evolution is essentially passive, except possibly for minor mergers, giving raise to observables such as the comoving space density and the composition of the stellar population resembling those expected according to the “monolithic” scenario.

As mentioned by Granato et al. (2001), two distinctive features are predicted for SCUBA/MAMBO galaxies, which are the subject of the present work. The first one is that those galaxies are highly biased tracers of the matter distribution, and that well defined links are established between these galaxies and other galaxy populations such as Lyman Break Galaxies (LBGs) and Extremely Red Objects (EROs), and with AGNs. The second feature is the extremely steep, essentially exponential decline of the bright tail of (sub)-mm counts.

Studies of clustering properties are particularly challenging in this scenario; if different objects are drawn from the same population of sources they have to exhibit the same large-scale (and therefore clustering) behaviour. In this context, it is interesting to note that Almaini et al. (2002) have found that SCUBA galaxies and Chandra sources (which are mostly AGNs), although showing a small direct overlap, have essentially the same projected distribution on the sky, suggesting an evolutionary connection between the two populations. Hints that LBGs may indeed be the lower luminosity/lower mass counterparts to SCUBA sources, as argued by Granato et al. (2001), come from the findings that the most intrinsically luminous LBGs, presenting the highest star-formation rate, contain more dust (Pettini et al. 2001) and have stronger clustering (Giavalisco & Dickinson 2001), and that there is a strong cross-correlation among the two populations (Webb et al. 2002a). A first discussion of these issues was offered by Magliocchetti et al. (2001a, henceforth MA2001). In this paper we extend the analysis in two main aspects: (i) the clustering predictions are compared with observational data at 850 and 170 μm , (ii) the clustering contribution to fluctuations in the background radiation is computed and compared with that of the cosmological signal as well as of the Galactic dust emission.

While clustering deals with the statistics of spatial distribution of Spheroids, another most relevant aspect is the predicted distribution in fluxes of these sources, since as we mentioned above they are predicted to have an extremely steep, essentially exponential decline of the bright tail of mm/sub-mm counts. This is due to the fact that, according to the adopted model, the bulk of star formation in such objects is essentially complete at $z \simeq 2$. The bright counts therefore essentially reflect the high luminosity tail of the luminosity function. This in turn relies on the fact that within the hierarchical clustering scenario massive halos are exponentially rare at high redshifts. Hints of such a steep decline can possibly be discerned in the recent MAMBO (Carilli et al. 2001; Bertoldi et al. 2000) and SCUBA bright surveys (Scott et

al. 2001; Borys et al. 2001).

In the present work we extensively discuss the implications of this aspect on the amount of sources which undergo amplifications due to strong gravitational lensing, focusing on the effect on number counts for fluxes $10\text{mJy} \lesssim S_{850\mu\text{m}} \lesssim 100\text{mJy}$. We show in particular how the fraction of strongly lensed objects with respect to all the contributing populations are generally much more copious than in other (phenomenological) models that also successfully account for SCUBA/MAMBO counts (Rowan-Robinson 2001; Takeuchi et al. 2001; Pearson et al. 2001). We conclude that the measure of the fraction of strongly lensed objects on (sub)-mm counts at the mentioned fluxes is a powerful test for confirming or rejecting the present scenario.

The layout of this paper is as follows. In § 2 we compare the predictions of the model by Granato et al. (2001) with recent measurements of clustering properties of SCUBA galaxies (Peacock et al. 2000; Scott et al. 2001; Webb et al. 2002b) and draw some conclusions on the cell-to-cell fluctuations of the projected density of sources, found to be strong enough to account for the discrepancies in the number counts observed in different regions of the sky by different groups. In § 3 we present the power spectra of total intensity fluctuations due to clustering of forming spheroidal galaxies in different PLANCK/HFI channels; we compare such spectra with those expected by Cosmic Microwave Background and Galactic dust emission (Finkbeiner et al. 1999) and derive predictions for the power spectrum of extragalactic background fluctuations at 170 μm , to be compared with the signal detected by Lagache & Puget (2000). § 4 gives the essential details of our calculations on the effect of lensing on source counts, while in § 5 we report our predictions for counts of lensed galaxies at mm/sub-mm wavelengths, with reference to those covered by the PLANCK/HFI instrument. Conclusions are presented in § 6.

Throughout the paper we will assume a Cold Dark Matter flat cosmology with $\Omega_\Lambda = 0.7$, $\Omega_b h^2 = 0.025$, $H_0 = 100h_0 \text{ km s}^{-1} \text{ Mpc}^{-1}$ with $h_0 = 0.7$ and a COBE-normalized $\sigma_8 = 1$. We note however that our conclusions are only weakly dependent on the underlying cosmological model.

2. CLUSTERING OF HIGH-Z FORMING SPHEROIDAL GALAXIES: MODEL PREDICTIONS VS. OBSERVATIONS

A crucial test for a galaxy formation model is its ability to correctly describe the large-scale properties of the populations under investigation. In MA2001 we have presented predictions for the clustering of SCUBA sources and their contribution to the total background fluctuations in the sub-mm band, based on the model by Granato et al. (2001). The model has been proven to provide a good fit to the clustering properties of LBGs (Giavalisco et al. 1998), corresponding in our framework to the early evolutionary phases of low-to-intermediate mass spheroidal galaxies.

In this Section we extend the analysis of MA2001 and compare the results to the best up-to-date clustering measurements at 850 μm . We start off with the theoretical expression for the angular two-point correlation function $w(\theta)$:

$$w(\theta) = 2 \frac{\int \int_0^\infty N^2(z) b_{\text{eff}}^2(M_{\text{min}}, z) (dz/dx) \xi(r, z) dz du}{[\int_0^\infty N(z) dz]^2} \quad (1)$$

(Peebles 1980), where $\xi(r, z)$ is the spatial mass-mass correlation function (obtained as in Peacock & Dodds 1996; see also Moscardini et al. 1998 and Magliocchetti et al. 2000), x is the comoving radial coordinate, $r = (u^2 + x^2 \theta^2)^{1/2}$ (for a flat universe and in the small angle approximation), and $N(z)$ is the

number of objects within the shell ($z, z + dz$). The relevant properties of SCUBA galaxies are included in the redshift distribution of sources $N(z)$, and in the bias factor $b_{\text{eff}}(M_{\text{min}}, z)$.

Trends for the predicted redshift distribution of sources respectively brighter than 1, 10 and 50 mJy are shown in Granato et al. (2001) and MA2001. Independent of the flux-limit adopted, all the curves feature a maximum at $z \simeq 3$, while the redshift range spanned progressively becomes narrower as one goes from fainter to brighter objects. We note that our predictions for a very limited number of sources ($\lesssim 10\%$ to 30%) to appear at redshifts $z \lesssim 2$ is in full agreement with all the available data (see e.g. Smail et al. 2000; Smail et al. 2002; Dunlop 2001a; Eales et al. 2000; Webb et al. 2002b).

The effective bias factor $b_{\text{eff}}(M_{\text{min}}, z)$ of all the dark matter haloes with masses greater than some threshold M_{min} is then obtained by integrating the quantity $b(M, z)$ (whose expression has been taken from Jing 1998) – representing the bias of individual haloes of mass M – weighted by the mass function $n_{\text{SCUBA}}(M, z)$ of SCUBA sources:

$$b_{\text{eff}}(M_{\text{min}}, z) = \frac{\int_{M_{\text{min}}}^{\infty} dM b(M, z) n_{\text{SCUBA}}(M, z)}{\int_{M_{\text{min}}}^{\infty} dM n_{\text{SCUBA}}(M, z)}, \quad (2)$$

with $n_{\text{SCUBA}}(M, z) = n(M, z) T_B/t_h$, where $n(M, z) dM$ is the mass function of haloes (Press & Schechter, 1974; Sheth & Tormen 1999), T_B is the duration of the star-formation burst and t_h is the life-time of the haloes in which these objects reside. Following Lacey & Cole (1993), this last quantity is defined as $t_h(M, z) = t_s(M, z) - t_u(z)$, where $t_s(M, z)$ is the survival time of a halo having a mass M at redshift z (i.e. the cosmic time by which the mass of such a halo has doubled either due to accretion or merging), and $t_u(z)$ is the age of the universe at an epoch corresponding to z .

The bias factor b_{eff} in Eq. (2) and the angular correlation function of Eq. (1) have then been evaluated for three mass ranges: i) masses in the range $M_{\text{sph}} \simeq 10^9 - 10^{10} M_{\odot}$, duration of the star formation burst $T_B \sim 2$ Gyr, and typical $850 \mu\text{m}$ fluxes $S \lesssim 1$ mJy; ii) masses in the range $M_{\text{sph}} \simeq 10^{10} - 10^{11} M_{\odot}$ and $T_B \sim 1$ Gyr; iii) masses in the range $M_{\text{sph}} \gtrsim 10^{11} M_{\odot}$, $T_B \sim 0.5$ Gyr, dominating the counts at $850 \mu\text{m}$ fluxes $S \gtrsim 5 - 10$ mJy (note that by M_{sph} we denote the mass in stars at the present time).

Furthermore, we considered two extreme values for the ratio between mass in stars and mass of the host dark halo – $M_{\text{halo}}/M_{\text{sph}} = 100$ and $M_{\text{halo}}/M_{\text{sph}} = 10$ – which encompass the range covered by recent estimates for massive objects (McKay et al. 2001; Marinoni & Hudson 2001). Granato et al. (2001) found that this ratio is about 20 to 30 for the massive objects.

According to our model, sources are expected to be strongly clustered, with a clustering signal which increases for brighter sources and higher values of $M_{\text{halo}}/M_{\text{sph}}$. From the above discussion it follows that measurements of $w(\theta)$ are in principle able to discriminate among different models for SCUBA galaxies and in particular to determine both their star-formation rate, via the amount of baryonic mass actively partaking of the process of star formation, and the duration of the star-formation burst.

In Fig. 1 the angular correlation functions predicted by our model are compared with the recent tentative evidence for positive clustering of SCUBA galaxies with $S(850 \mu\text{m}) \geq 5$ mJy (Scott et al. 2001) and with $S(850 \mu\text{m}) \geq 3$ mJy (Webb et al. 2002b). Although such measurements are dominated by noise due to the small-number statistics, they suggest the possibility that future larger sample may provide sharper tests for the models.

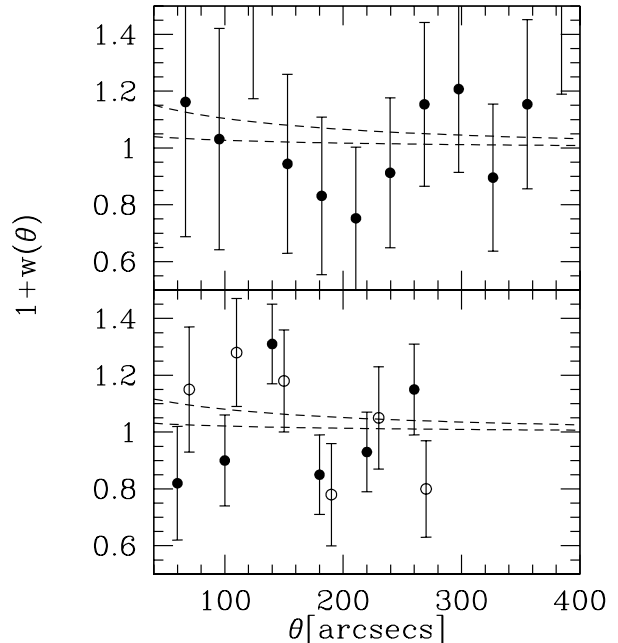


FIG. 1.—Top panel: angular correlation function of $S \geq 5$ mJy SCUBA sources. Model predictions are shown by the dashed curves (where the higher one is for $M_{\text{halo}}/M_{\text{sph}} = 100$ and the lower one for $M_{\text{halo}}/M_{\text{sph}} = 10$), while data points represent the Scott et al. (2001) measurements. Bottom panel: same as above but for sources brighter than 3 mJy. Data are taken from Webb et al. (2002b); empty and filled circles represent measurements obtained in two different fields of the Canada-UK Deep Submillimeter Survey (CUDSS).

Peacock et al. (2000) analyzed the contribution of clustering of unresolved ($S < 2$ mJy) SCUBA sources to the $850 \mu\text{m}$ background fluctuations detected in the Hubble Deep Field (HDF) North. They found some evidence for clustering of the background source population, consistent with an angular correlation function of the form $w(\theta) = (\theta/\theta_0)^{-pd_{\text{filon}}}$, for an a priori value of $pd_{\text{filon}} = 0.8$ and $\theta_0 = 1''$. Figure 2 presents our model predictions for the angular correlation function $w(\theta)$ derived in the case of SCUBA galaxies with $S < 2$ mJy; the redshift distribution spans the range $0.7 \lesssim z \lesssim 6$.

Our results are fully consistent with the constraints on structure in the sub-millimeter background set by Peacock et al. (2000) and not far from their preferred clustering model (dotted line in Fig. 2), if $M_{\text{halo}}/M_{\text{sph}} = 100$. The shallower slope predicted by our model at small angles ($\theta \lesssim 4 \times 10^{-2}$ degrees) ultimately stems from the fact that at high z we enter the regime of linear growth of density perturbations. This entails a flattening of the slope of the two-point spatial correlation function $\xi(r, z)$ for $z \gtrsim 2$. As a consequence, the angular correlation function $w(\theta)$ obtained as in Eq. (1) by projecting $\xi(r, z)$ over a wide range of redshifts, up to $z \simeq 6$, will mirror this tendency to flatten out. On the other hand, we cannot exclude the presence of a non-linear and/or scale-dependent bias (see e.g. Dekel & Lahav 1999; Blanton et al. 1999; Narayanan et al. 2000) at the small physical scales probed by the Peacock et al. (2000) sample, which could raise the slope of the angular correlation function up to values closer to the standard -0.8 .

Strong clustering substantially enhances cell-to-cell fluctuations of the surface density of detected sources. The angular correlation function $w(\theta)$ is in fact related to the second moment (variance) of the galaxy distribution function via the expression

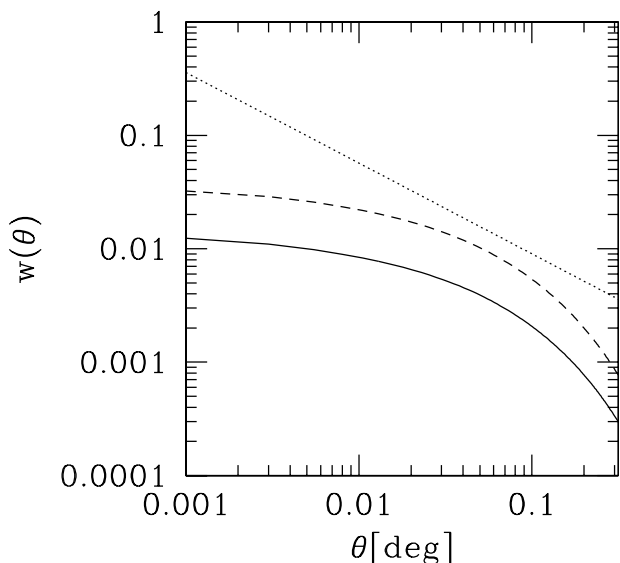


FIG. 2.—Angular clustering of unresolved ($S < 2$ mJy) sources at $850\mu\text{m}$. The solid curve is obtained for $M_{\text{halo}}/M_{\text{sph}} = 10$, while the dashed one represents the case $M_{\text{halo}}/M_{\text{sph}} = 100$. The dotted line corresponds to $w(\theta) = (\theta/1'')^{-0.8}$ (Peacock et al. 2000).

(Peebles 1980; Roche & Eales 1999):

$$\mu_2 = \bar{N} + \left(\frac{\bar{N}}{\omega}\right)^2 \Sigma^2, \quad (3)$$

where \bar{N} – mean count of sources in the solid angle ω – represents the Poisson noise arising from the discrete nature of the objects, and the normalized variance Σ^2 can be written as

$$\Sigma^2 = \int w(\theta) d\omega_1 d\omega_2. \quad (4)$$

In the case of square cells with $\omega = \Theta \times \Theta$, Eq. (4) can be expressed as the two-dimensional integral

$$\Sigma^2(\Theta) = \Theta^2 \int_0^\Theta dx \int_0^\Theta w(\theta) dy, \quad (5)$$

with $\theta = \sqrt{x^2 + y^2}$.

The quantity in Eq. (5) has been evaluated for the three cases of low-, intermediate- and high-mass SCUBA galaxies, introduced in this Section and based on the Granato et al. (2001) model, and for the usual two different values of the $M_{\text{halo}}/M_{\text{sph}}$ ratio. Results for the rms fluctuations relative to the mean number of detected sources per cell, $\mu_2^{1/2}/\bar{N}$ [see Eq. (3)] are presented in Fig. 3, where dashed and dotted curves respectively correspond to sources brighter than 10 and 1 mJy. We have adopted a mean surface density per square degree of $\bar{N} = 180$ for a flux limit of 10 mJy, (see Scott et al. 2001), and of $\bar{N} = 1.3 \times 10^4$ for a flux limit of 1 mJy (Granato et al. 2001). Fig. 3 clearly illustrates that the contributions to cell-to-cell fluctuations due to clustering are generally at least comparable to, and may be much larger than the Poisson ones, shown by the two solid lines. We therefore conclude that the high clustering amplitude predicted for SCUBA sources can easily account for the differences found in the number counts observed in different sky regions by different groups (see e.g. Smail et al. 1997;

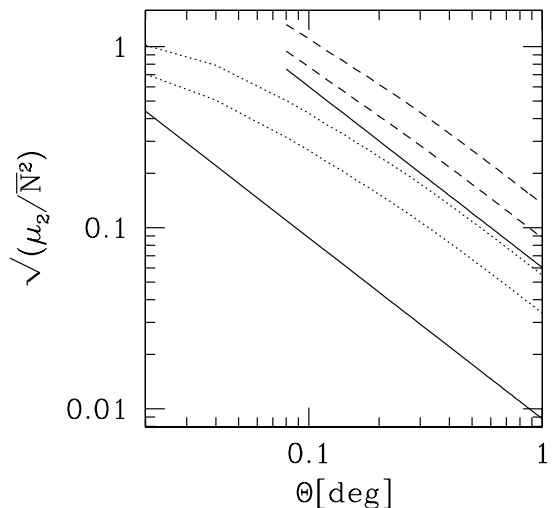


FIG. 3.—Predictions for the rms fluctuations relative to the mean number of detected sources per cell of area $\omega = \Theta^2$, $\mu_2^{1/2}/\bar{N}$, at $850\mu\text{m}$. Dashed and dotted lines are for sources brighter than 10 mJy or 1 mJy, respectively. Higher curves of each type correspond to $M_{\text{halo}}/M_{\text{sph}} = 100$, lower ones to $M_{\text{halo}}/M_{\text{sph}} = 10$. The solid lines show the Poisson contributions for the two flux limits. The lines are drawn only for angular scales such that the mean number of source in the solid angle $\omega = \Theta^2$ is > 1 .

Hughes et al. 1998; Blain et al. 1999; Barger et al. 1999a; Eales et al. 2000; Scott et al. 2001). On the other hand, currently available samples are too small to allow an unambiguous recognition of the effect of clustering. From Eq. (3) we estimate that an observational determination of the cell-to-cell variance due to clustering, as predicted by the model, would require a survey of a few $\times 10^{-2} \text{ deg}^2$ if the source detection limit is 1 mJy and of $\simeq 1 \text{ deg}^2$ for a detection limit of 10 mJy.

3. MULTI-WAVELENGTH ANALYSIS OF THE CONTRIBUTION OF CLUSTERING TO BACKGROUND FLUCTUATIONS

The strong clustering of high- z forming spheroidal galaxies adds an important contribution to background fluctuations. Measurements of such a contribution can be informative on both the nature and the properties of sources below the detection limit. On the other hand, these fluctuations may have a significant impact on the detectability of Cosmic Microwave Background (CMB) fluctuations.

MA2001 (but see also Scott & White 1999 and Haiman & Knox 2000) estimated the power spectrum of clustering fluctuations at $850\mu\text{m}$. In the present Section we apply the same analysis to different wavelengths, corresponding to the effective frequencies of the channels of the High Frequency Instrument (HFI) of the PLANCK ESA mission: $2100\mu\text{m} \rightarrow 143 \text{ GHz}$; $1380\mu\text{m} \rightarrow 217 \text{ GHz}$; $550\mu\text{m} \rightarrow 545 \text{ GHz}$; $350\mu\text{m} \rightarrow 857 \text{ GHz}$. We also work out predictions at $\lambda = 170\mu\text{m}$, the wavelength probed by the FIRBACK deep survey (Dole et al. 2001).

The counts of spheroidal galaxies are obtained from the model by Granato et al. (2001). The counts of spiral and star-burst

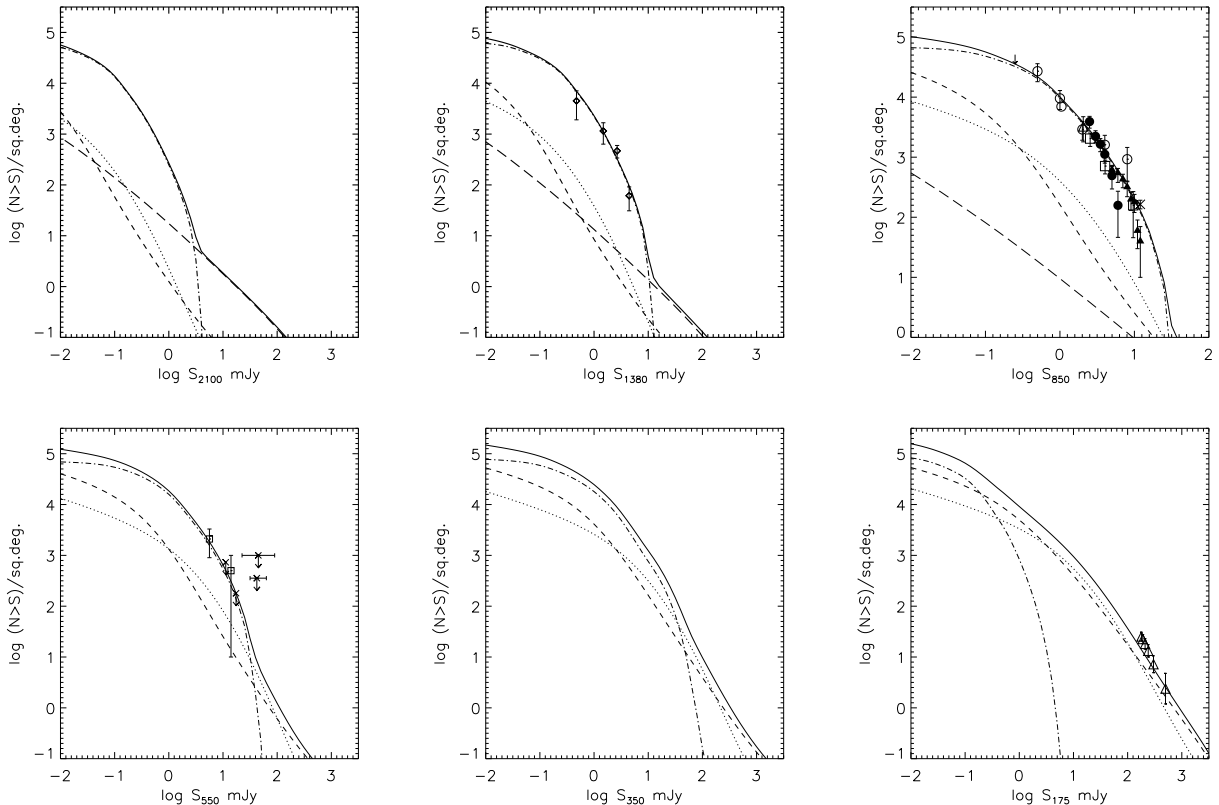


FIG. 4.—Integral number counts of galaxies predicted by the model of Granato et al. (2001) at $\lambda = 2100\mu\text{m}$ (top left-hand panel), $\lambda = 1380\mu\text{m}$ (top middle panel), $\lambda = 850\mu\text{m}$ (top right-hand panel), $\lambda = 550\mu\text{m}$ (bottom left-hand panel), $\lambda = 350\mu\text{m}$ (bottom middle panel) and $\lambda = 175\mu\text{m}$ (bottom right-hand panel). The solid lines show the total counts while the dot-dashed, dashed, and dotted lines are respectively obtained for the three populations of forming spheroidals, of spirals and of star-burst galaxies. The long-dashed lines (only for $\lambda \geq 850\mu\text{m}$) show the counts of radio sources, based on the model by Toffolatti et al. (1998). Data in the $1380\mu\text{m}$ panel are derived from MAMBO observations (Bertoldi et al., 2001); a flux density ratio $S_{1200}/S_{1380} = 1.5$ has been adopted to extrapolate to $\lambda = 1.38\text{ mm}$ the MAMBO flux densities at $\lambda = 1.2\text{ mm}$ (according to the model, such ratio varies between 1.4 and 1.6, depending on the details of the dust temperature distribution). Data at $175\mu\text{m}$ are from Dole et al. (2001). Data at $850\mu\text{m}$ are from Blain et al. (1999) (open circles), Hughes et al. (1998) (open triangles), Barger et al. (1999) (open squares), Eales et al. (2000) (filled circles), Scott et al. (2001) (filled triangles), Borys et al. (2001) (crosses). Data at $550\mu\text{m}$ are an extrapolation of the $450\mu\text{m}$ observations by Blain et al. (2000), Barger et al. (1998), Smail et al. (1997); Hughes et al. (1998), Eales et al. (1999); a mean ratio $S(450\mu\text{m})/S(550\mu\text{m}) = 1.78$, typical for spiral and starburst galaxies, has been adopted.

galaxies at all the wavelengths relevant to this work have been instead estimated by extrapolating the $60\mu\text{m}$ local luminosity functions of these two populations (Saunders et al. 1990), and evolving them in luminosity as $L(z) = L(0)(1+z)^\alpha$, with $\alpha = 3.5$ in the case of starbursts and $\alpha = 0$ for spirals. The extrapolation in frequency has been carried out adopting the observed spectral energy distributions of NGC6946 and NGC6090, respectively in the case of spirals and star-burst galaxies (see Silva et al. 1998). No evolution is assumed for spiral galaxies in keeping with the notion of almost constant star-formation rate in discs, at least in the last 6–7 Gyr, corresponding to $z \leq 0.5$. The evolution of the starburst population, i.e. $\alpha = 3.5$, is instead fixed by the fits to the 175 and $60\mu\text{m}$ counts. It is worth noticing that the starburst and spiral counts at $S_{850} \geq 5\text{--}10\text{ mJy}$ are almost fixed by the observed $175\mu\text{m}$ counts.

The contribution to the counts of forming spheroidal galaxies, compared to that of spiral and star-burst galaxies, is found to decrease for decreasing wavelength because of the increasingly less favorable K-corrections associated with the former population. Spirals and starbursts consequently become more and more important at shorter and shorter wavelengths, and eventually dominate the counts for $\lambda \lesssim 200\mu\text{m}$. This is illustrated by Fig. 4, where we show the contribution to the integral number

counts (represented by the solid curves) of the three populations of spheroidal galaxies (dot-dashed lines), spirals (dashed lines) and starbursts (dotted lines) at different wavelengths.

Figure 4 shows that – under our assumptions – star-bursts and spirals constitute a negligible fraction of the total number of sources at mm/sub-mm wavelengths, the dominant contribution coming from high- z forming spheroidal galaxies (the same which – according to Granato et al. 2001 – show up as SCUBA sources at $\lambda = 850\mu\text{m}$), at all but very bright fluxes (with a flux threshold which varies with wavelength) where, as already discussed in the introduction and extensively tackled in Section 4, the number counts of spheroidal galaxies experience an exponential decline. The situation is reversed at $175\mu\text{m}$ (bottom right panel of Figure 4) where, down to fluxes $S_{175\mu\text{m}} \simeq 0.3\text{ mJy}$, spirals and star-bursts dominate the predicted number counts. In the following analysis we will therefore only consider the population of spheroidal galaxies when dealing with the mm/sub-mm wavelength range.

The angular correlation function of intensity fluctuations due to inhomogeneities in the space distribution of unresolved sources (i.e. with fluxes fainter than some threshold S_d), $C(\theta)$, can be expressed as the sum of two terms C_P and C_C , the first one due to Poisson noise (fluctuations given by randomly dis-

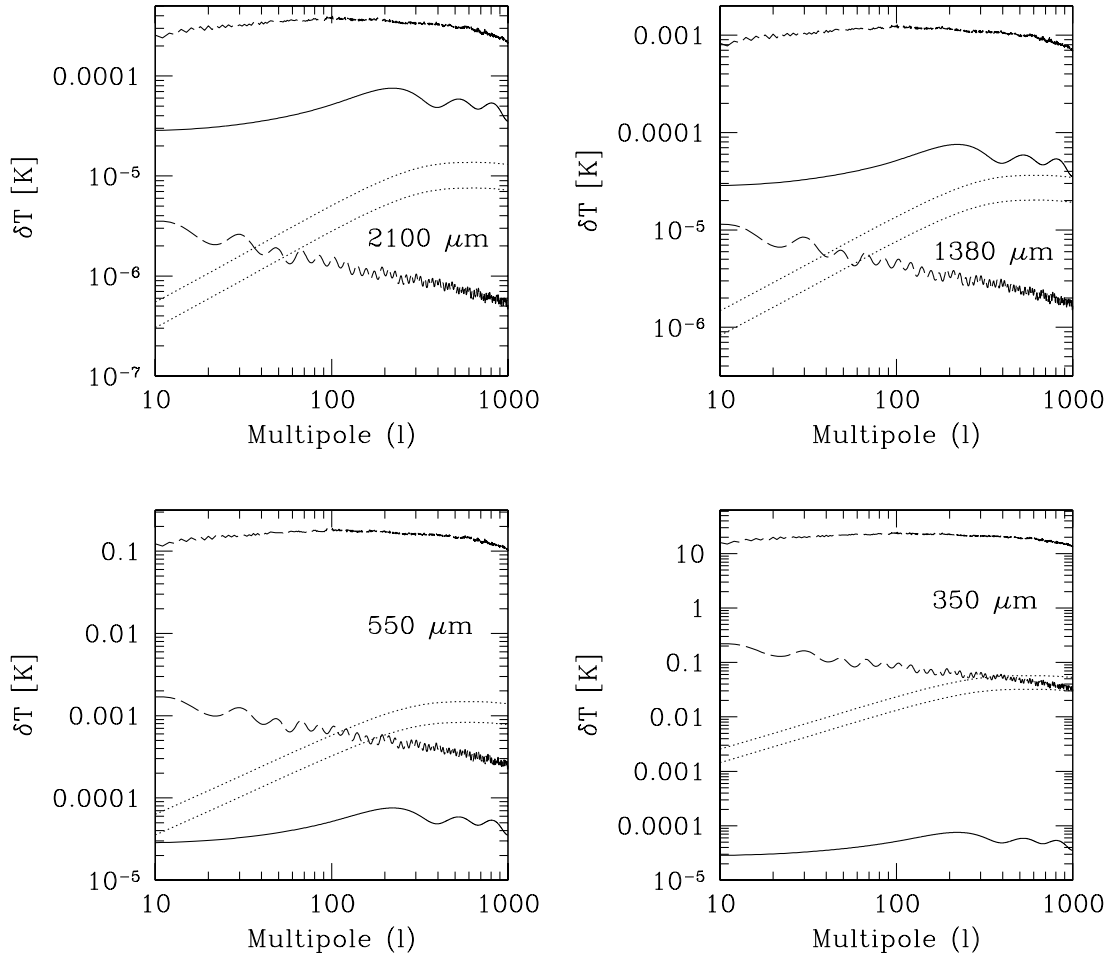


FIG. 5.—Predicted power spectrum of temperature fluctuations $\delta T_l = \sqrt{l(l+1)C_l/2\pi}$ (in units of K) as a function of the multipole l at $2100 \mu\text{m}$ (top-left panel), $1380 \mu\text{m}$ (top-right panel), $550 \mu\text{m}$ (bottom-left panel) and $350 \mu\text{m}$ (bottom-right panel), central frequencies of the PLANCK/HFI channels. The dotted curves are for the 5σ flux detection limit of each channel. Higher curves of the same kind are for $M_{\text{halo}}/M_{\text{sph}}=100$, lower ones for $M_{\text{halo}}/M_{\text{sph}}=10$. The solid lines represent the power spectrum of primary CMB anisotropies as predicted by a standard Λ CDM cosmology ($\Omega_\Lambda = 0.7$, $\Omega_0 = 0.3$, $h_0 = 0.7$). The upper long-dashed curves represent the contribution from Galactic dust emission averaged all over the sky, while the lower ones correspond to high galactic latitudes ($|b| \geq 80^\circ$) only. The clustering signal is potentially detectable at several wavelengths by a high sensitivity experiment like PLANCK/HFI in regions of low Galactic dust emission, particularly after application of efficient component separation algorithms. Its contamination of CMB maps is however small at $2100 \mu\text{m}$ and at $1380 \mu\text{m}$ may be important only on small scales. On the other hand, foregrounds dominate over the CMB for $\lambda \leq 550 \mu\text{m}$.

tributed objects), and the second one owing to source clustering (see MA2001 and De Zotti et al. 1996 for a detailed discussion). In the case of highly clustered sources such as forming spheroidal galaxies, the Poisson term C_P is found (see e.g. Scott & White 1999) to be negligible when compared to C_C . We can therefore safely assume $C \simeq C_C$, whose expression is given by

$$C_C(\theta) = \left(\frac{1}{4\pi}\right)^2 \int_{z(L_{\min}, S_d)}^{z_{\max}} dz b_{\text{eff}}^2(M_{\min}, z) \frac{j_{\text{eff}}^2(z)}{(1+z)^4} \left(\frac{dx}{dz}\right)^2 \cdot \int_0^\infty d(\delta z) \xi(r, z), \quad (6)$$

with $b_{\text{eff}}(M_{\min}, z)$ defined by Eq. (2), x being the comoving radial coordinate, $\delta z = c/H_0 u$ (u is introduced in Eq. (1) and c is the speed of light), z_{\max} the redshift when the sources begin to shine, $z(S_d, L)$ the redshift at which a source of luminosity L is seen with a flux equal to the detection limit S_d and j_{eff} is the effective volume emissivity.

Following the MA2001 approach, $C_C(\theta)$ in Eq. (6) has then been evaluated separately for the three cases of low-, intermediate- and high-mass objects, and the total contribution of clustering to intensity fluctuations $C^{TOT}(\theta)$ has been derived by adding up in quadrature all the values of $C_C(\theta)$ obtained for the different mass intervals and by also taking into account the cross-correlation terms between objects of different masses.

The angular power spectrum of the intensity fluctuations can then be obtained as

$$C_l = \langle |a_l^0|^2 \rangle = \int_0^{2\pi} \int_0^\pi [\delta T(\theta)]^2 P_l(\cos\theta) \sin\theta d\theta d\phi, \quad (7)$$

with

$$\delta T(\theta) = \langle (\Delta T)^2 \rangle^{1/2} = \frac{\lambda^2 \sqrt{C^{TOT}(\theta)}}{2k_b} \left[\exp\left(\frac{h\nu}{k_b T}\right) - 1 \right]^2 \cdot \exp\left(-\frac{h\nu}{k_b T}\right) / \left(\frac{h\nu}{k_b T}\right)^2, \quad (8)$$

which relates intensity and brightness total intensity fluctuations.

This analysis has been performed for the different central frequencies of the PLANCK HFI, and Figure 5 shows the results in terms of $\delta T_l = \sqrt{l(l+1)C_l/2\pi}$ (in units of K) at 2100 μm , 1380 μm , 550 μm and 350 μm . In each of the four panels of Fig. 5, dotted curves are obtained by adopting the 5σ detection limits of the different PLANCK channels ($S_{\text{lim}} = 300$ mJy at 2100 μm ; $S_{\text{lim}} = 200$ mJy at 1380 μm ; $S_{\text{lim}} = 450$ mJy at 550 μm ; $S_{\text{lim}} = 700$ mJy at 350 μm) estimated by Toffolatti et al. (1998). In Figure 6 we also plot predictions for temperature fluctuations at 850 μm , where the contribution from star-forming spheroidals has been corrected for a programming mistake affecting the numerical calculations by MA2001, which produced wiggles in the trend of the predicted power spectrum for multipoles $l \gtrsim 200$. The dotted curves are obtained for a source detection limit of $S_{\text{lim}} = 100$ mJy, while the dashed ones illustrate the case of a ten times higher sensitivity ($S_d = 0.1 S_{\text{lim}}$). Note the very weak dependence of the clustering signal on the detection limit, as far as it lays in the steep portion of the counts, implying that the results shown in Figure 6 are representative also in the case of surveys with detection limits higher than 100 mJy, as is probably the case for the Planck mission. On the other hand, other forthcoming large area surveys (see, e.g., the BLAST project, Devlin et al. 2000; www.hep.upenn.edu/blast/) can go substantially deeper than PLANCK over limited areas of the sky.

The solid curves in Figs. 5 and 6 show, for comparison, the power spectrum of primary Cosmic Microwave Background (CMB) anisotropies corresponding to a flat Λ CDM cosmology, calculated with the CMBFAST code developed by Seljak & Zaldarriaga (1996). The relative importance of fluctuations due to clustering rapidly increases with decreasing wavelength. CMB anisotropies on small angular scales are exceeded at all wavelengths $\lambda \leq 850 \mu\text{m}$. This high clustering signal mostly comes from massive galaxies with bright fluxes, which lie at substantial redshifts and are therefore highly biased tracers of the underlying mass distribution. Also the negative K-corrections increase their contribution to the effective volume emissivity (see MA2001) and therefore to the fluctuations.

This implies that important information on the clustering properties of faint sub-mm/far-IR galaxies (and hence on physical properties such as their mass and/or the amount of baryons involved in the star-formation process) will reside in the PLANCK maps at frequencies greater than 353 GHz where, however, the dominant diffuse signal at those frequencies is expected to come from interstellar dust emission.

In order to quantify this last effect, we have calculated the expected contribution of Galactic dust emission to background fluctuations. To this end, the full-sky dust emission maps at sub-millimeter and microwave wavelengths constructed by Finkbeiner et al. (1999) from IRAS and COBE (DIRBE and FIRAS) data, have been used.

Fig. 5 shows the power spectrum of Galactic dust emission averaged all over the sky (upper long-dashed curves). This signal dominates at all wavelengths due to the large contribution from the Galactic plane. However, it is still possible to detect the clustering signal of sub-mm galaxies (and also recover the CMB power spectrum for $\lambda \gtrsim 10^3 \mu\text{m}$) if one restricts the analysis to low-dust regions, e.g. to high enough Galactic latitude regions (i.e. $|b| \geq 80^\circ$, lower long-dashed curves).

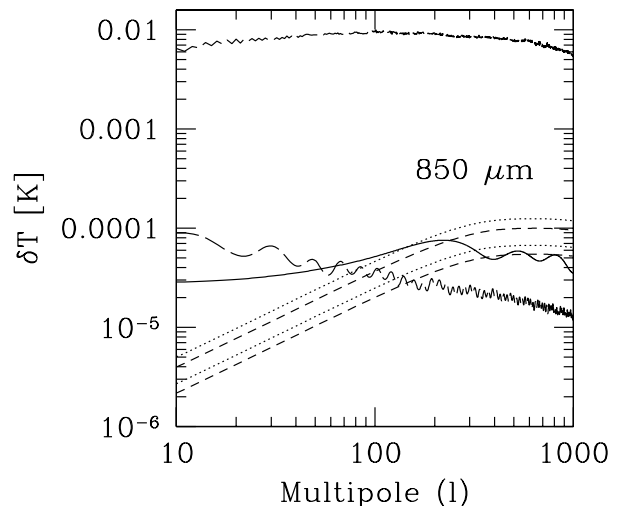


FIG. 6.—As in Figure 5, but for the 850 μm case. Dotted lines are for a detection limit $S_d = 100$ mJy while dashed ones for $S_d = 10$ mJy. Higher curves of the same kind are for $M_{\text{halo}}/M_{\text{sph}}=100$, lower ones for $M_{\text{halo}}/M_{\text{sph}}=10$.

It turns out that, both for $\lambda = 850 \mu\text{m}$ (see also Magliocchetti et

al. 2001b) and $\lambda = 550\mu\text{m}$, the dust contribution in these regions becomes less important than the one due to the clustering of unresolved sources at any $l \gtrsim 100$. For $\lambda = 350\mu\text{m}$ the signal due to Galactic dust is instead found to hide all the other sources of background fluctuations at all Galactic latitudes, except possibly in the case of very high ($l \gtrsim 800$) multipoles.

Background fluctuations due to unresolved extragalactic sources have recently been measured by Lagache & Puget (2000) at $170\mu\text{m}$ in a field covered by the FIRBACK survey with ISOPHOT (Dole et al. 2001). As already mentioned, in this case the dominant contribution to counts and to small-scale fluctuations is expected, according to our model, to come from low-to-intermediate-redshift spiral and starburst galaxies, whose bias factor $b_{\text{eff}}(M_{\text{min}}, z)$ appearing in Eq. (6) takes the form:

$$b(z) = 1 + \frac{b_0 - 1}{D(z)} \quad (9)$$

(Fry 1996; see also Baugh et al. 1999; Magliocchetti et al. 1999; Magliocchetti et al. 2000), independent of the mass of the haloes hosting such sources and merely a function of redshift – via the linear growth rate $D(z)$ – and of the local bias $b_0 \equiv b(z=0) = \sigma_{8,\text{gal}}/\sigma_8$, where $\sigma_{8,\text{gal}}$ is the rms fluctuation amplitude in a sphere of radius $8\text{ h}^{-1}\text{Mpc}$ as measured in the local universe for each population. We have estimated the amplitudes $\sigma_{8,g}$ from the clustering properties by spectral type determined by Loveday, Tresse & Maddox (1999) from Stromlo-APM survey data. We find $\sigma_{8,g} = 0.93$ for galaxies with weak emission lines (spirals) and $\sigma_{8,g} = 0.66$ for galaxies with strong emission lines (starbursts).

The contribution of clustering to $C(\theta)$ has then been calculated for the three populations of spheroidals, spirals and starbursts and the angular power-spectrum $\Delta^2(k)$ has been derived according to the expression (see Peacock 1997):

$$\Delta^2(k) = k^2 \int_0^\infty C(\theta) J_0(k\theta) \theta d\theta, \quad (10)$$

where k is the angular wavenumber and J_0 is the zero-th order Bessel function. The results for a detection limit $S_d = 135\text{ mJy}$, corresponding to three times the confusion noise of the FIRBACK survey (Dole et al. 2001), are shown in Fig. 7. As expected, the contribution of spheroidal galaxies at this wavelength is negligible when compared to those originating from the clustering of both star-burst galaxies and spirals. Also, despite the strongly negative bias, the signal obtained for starbursts turns out to be stronger than the one predicted for spiral galaxies, due to the different evolutionary properties of the two populations, as outlined above.

The short/long-dashed curve in Figure 7 represents the Poisson contribution $P_P = 7400\text{ Jy}^2/\text{sr}$ derived from the Guiderdoni et al. (1997) predictions, while the dashed-dotted curve illustrates the contribution to the observed power-spectrum of the Galactic cirrus (Lagache & Puget 2000). According to our predictions, fluctuations stemming from the clustering of starburst galaxies are detectable above other sources of signal in the wavenumber range $0.04 \lesssim k \text{ (arcmin}^{-1}\text{)} \lesssim 0.3$.

4. GRAVITATIONAL LENSING

It is now well established (Franceschini et al. 1991, 1994, 2001; Blain & Longair 1993; Pearson & Rowan-Robinson 1996; Guiderdoni et al. 1997, 1998; Dwek et al. 1998; Blain et al. 1999; Devriendt & Guiderdoni 2000; Pearson et al. 2001; Takeuchi et al. 2001; Rowan-Robinson 2001) that the coupling of the strongly negative K-correction at mm/sub-millimetre

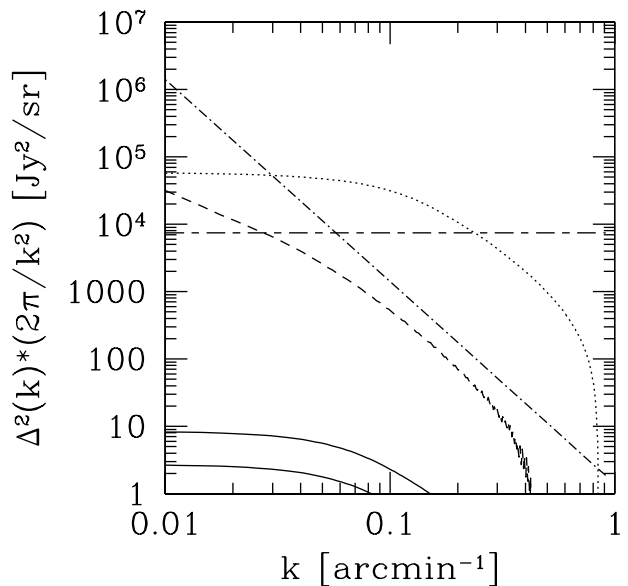


FIG. 7.—Predictions for the power-spectrum of intensity fluctuations due to clustering of galaxies fainter than a detection limit $S_d = 135\text{ mJy}$ at $\lambda = 170\mu\text{m}$. The solid curves are for the population of spheroidal galaxies (the higher one referring to $M_{\text{halo}}/M_{\text{sph}} = 100$, the lower one to $M_{\text{halo}}/M_{\text{sph}} = 10$), while the dashed and dotted curves respectively show the predictions for spiral and star-burst galaxies. The short/long-dashed curve represents a white noise power spectrum $P_P = 7400\text{ Jy}^2/\text{sr}$, while the dashed-dotted one illustrates the cirrus confusion noise (both from Lagache & Puget, 2000).

wavelengths – due to the steep increase with frequency of dust emission in galaxies – with the strong cosmological evolution demonstrated by both ISO and SCUBA data (Elbaz et al. 1999; Smail et al. 1997; Hughes et al. 1998; Barger et al. 1999a; Eales et al. 2000) and by the intensity of the far-IR background (Puget et al. 1996; Fixsen et al. 1998; Schlegel et al. 1998; Hauser et al. 1998; Lagache et al. 1999, 2000), greatly emphasizes high-redshift sources. This yields very steep counts which maximize the magnification bias and lead to a high probability for such sources to be gravitationally lensed (Peacock 1982; Turner et al. 1984). As already discussed by Blain (1996, 1997, 1998a,b, 1999, 2000), this corresponds to a fraction of lensed sources expected to show up in the mm/sub-millimetre band which is much larger than what is found in surveys at other wavelengths. For instance, Blain (1998a) predicts about 0.6 to 5% of the point sources observed in the future by the High Frequency Instrument (HFI) on board of the ESA satellite PLANCK to be lensed.

As first noted in Perrotta et al. (2002), a distinctive feature of the astrophysically grounded model by Granato et al. (2001) is that both the lensing probability and the magnification bias at mm/sub-mm wavelengths are substantially higher than those implied by other current, mostly phenomenological, models which also successfully account for SCUBA/MAMBO counts (Rowan-Robinson 2001; Takeuchi et al. 2001; Pearson et al. 2001). This is because, according to this model, most galaxies detected in blank-field SCUBA and MAMBO surveys are interpreted as massive ellipticals at $z \gtrsim 2$, in the process of building their stellar populations with very high star-formation rates (typically from a few hundreds to $\sim 1000\text{ M}_\odot\text{ yr}^{-1}$). Thus, on one side, the optical depth to lensing is, on average, significantly higher than for most of the other models, which generally predict a substantial fraction of objects to be at $z < 2$. On the other side, the model

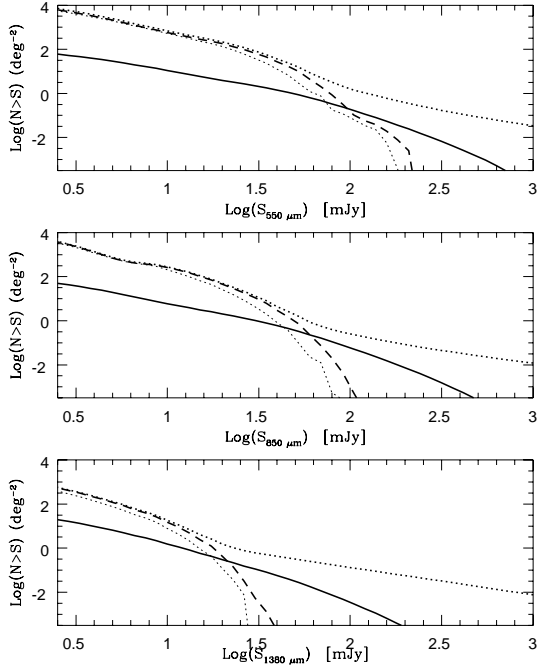


FIG. 8.—Integral source counts per square degree for the model by Granato et al. (2001) at 550 (top), 850 (middle) and 1380 μm . The dashed lines and the solid lines respectively refer to the weakly lensed (including the case of flux de-magnification) and strongly lensed counts of forming spheroids only; the light dotted line shows, for comparison, the counts of such sources as predicted by the model without taking lensing into account. The heavy dotted lines show the total counts after allowing for the effect of lensing on the counts of forming spheroids and including contributions from populations whose counts are essentially unaffected by lensing (such as “flat”-spectrum radio sources), as described in the text.

entails an extremely steep, essentially exponential, decline of the bright tail of mm/sub-mm counts of this galaxy population due to the fact that dust emission from these objects rapidly fades away at $z \lesssim 2$ when the bulk of their star formation is essentially over (Cohen 2001). The bright counts therefore somehow reflect the high luminosity tail of the luminosity function which, in turn, reflects the fact that, in the hierarchical clustering scenario, massive halos are exponentially rare at high redshifts (note that a similar redshift distribution for the SCUBA sources and similar source counts have been obtained in the parametric model of Blain et al. 1999, with an empirical approach).

Such a steep decrease of the number counts for fluxes $10\text{mJy} \lesssim S_{850\mu\text{m}} \lesssim 100\text{mJy}$ implies a large fraction of strongly lensed galaxies to appear at bright mm/sub-mm fluxes. Indeed, in Perrotta et al. (2002) we have shown that strongly lensed spheroids counts actually come to dominate the unlensed ones at fluxes of about 100 mJy, and at 850 μm wavelength. We provide here a detailed assessment of this promising result, quantifying the fraction of strongly lensed (sub)-mm sources when taking into account all the contributing populations at different wavelengths and giving a quantitative comparison with phenomenological models successfully accounting for SCUBA/MAMBO counts.

Let us first recall the main aspects of our model for gravitational lensing, referring to our previous work (Perrotta et al. 2002) for details. Lensing statistics is expressed by the probability for a source at redshift z_s to be lensed with magnification $> \mu$: it is obtained by dividing the total lensing cross section by

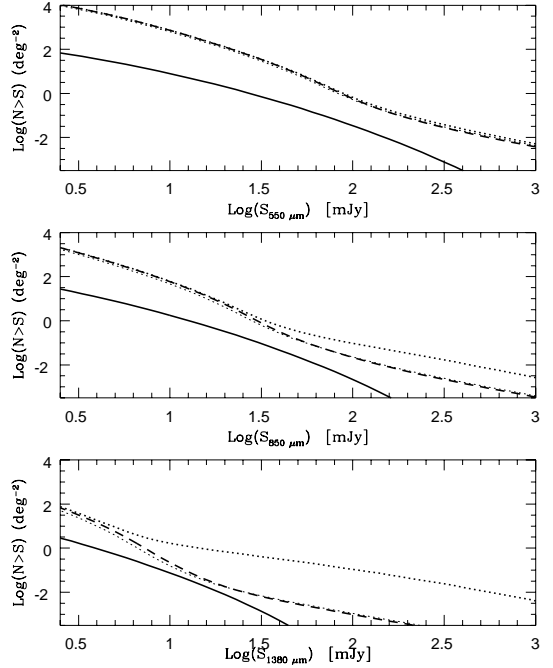


FIG. 9.—Integral source counts for the model by Rowan-Robinson (2001). The meaning of the lines is analogous to that in Fig. 8. In this case, however, the light dotted, the dashed (almost superimposed to the dotted), and the solid lines include the contributions of all the populations considered by Rowan-Robinson. The heavy dotted line also includes “flat”-spectrum radio sources for which the effect of lensing is negligible.

the area of the source sphere as

$$P(\mu, z_s) = \frac{(1+z_s)^2}{4\pi r^2(z_s)} \int_0^{z_s} dz \frac{dV}{dz} (1+z)^3 \times \int dM \sigma(\mu, z, z_s, M) \frac{dn}{dM}(z, M), \quad (11)$$

where $r(z)$ is the comoving radial distance to redshift z , dV/dz is the proper volume element per unit redshift, and $dn(z, M)/dM$ the comoving number density of the lenses. Since we are dealing with gravitational lensing by dark matter haloes, we assume that the lens distribution follows the Sheth & Tormen (1999) mass function

$$\frac{dn}{dM} = \sqrt{\frac{2aA^2}{\pi}} \frac{\rho_0}{M^2} \frac{\delta_c(z)}{\sigma(M)} \left[1 + \left(\frac{\sigma(M)}{\sqrt{a}\delta_c(z)} \right)^{2p} \right] \times \left| \frac{d \ln \sigma}{d \ln M} \right| \exp \left(-\frac{a\delta_c^2(z)}{2\sigma(M)^2} \right), \quad (12)$$

where the best-fit values of the parameters for our cosmological model are $a = 0.707$, $p = 0.3$, and $A \simeq 0.3222$. ρ_0 is the mean mass density at a reference epoch t_0 , which we assume to be the present time, and σ^2 is the variance of linear density fluctuations at the present epoch, smoothed with a spherical top-hat filter $W_R(k)$ enclosing a mass M . $\delta_c^2(z)$ is the linear density contrast of an object virialising at z , linearly evolved to the present epoch.

Quite independent of the lens model, $P(\mu, z)$ decreases as μ^{-2} for $\mu \gg 1$, hence the high magnification tail of the probability per unit magnification can be written as $p(\mu, z) = -dP(\mu, z)/d\mu \propto a(z)\mu^{-3}$. Equation (11) assumes non-overlapping cross sections, which is satisfied in the $P \ll 1$ regime, i.e. when no more than

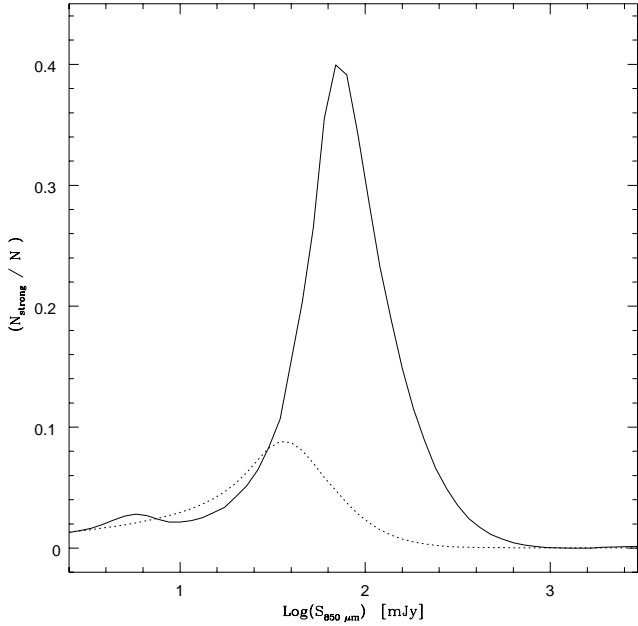


FIG. 10.—Ratio of strongly lensed to unlensed counts at 850 μm : the solid line refers to the model by Granato et al. (2001), the dotted line to the one by Rowan-Robinson (2001).

a single clump causes lensing of a background source: this results in magnifications markedly larger than 1, or strong lensing. Smaller magnifications, including de-magnifications, attain contributions from the distribution of dark matter along the entire line of sight, resulting in weak lensing effects. The latter case can be represented by a Gaussian probability per unit magnification:

$$p(\mu, z) = H(z) \exp[-(\mu - \bar{\mu})^2 / 2\sigma_\mu^2(z)]. \quad (13)$$

where the location of the peak, $\bar{\mu}$, and the amplitude, $H(z)$, are determined by the normalization and flux conservation conditions obtained by integrating over all possible magnifications the combined (weak plus strong lensing) probability distribution: $\int d\mu p(\mu, z) = \int d\mu \mu p(\mu, z) = 1$. The dispersion $\sigma_\mu(z)$ is discussed by Bartelmann & Schneider (2001). The transition between the weak and strong lensing regimes is set at a suitable magnification μ_{cut} : a convenient choice is $\mu_{\text{cut}} = 1 + 1.5\sigma_\mu(z)$, yielding $\mu_{\text{cut}} \approx 1.5 - 2$ for the redshift range of interest.

In the case of extended sources we must allow for a magnification cut-off, determined by the intrinsic brightness profile of the source (Peacock 1982), by the mass density profile of the lens, and by the geometry of the source/lens system. We follow the approach by Peacock (1982) and introduce a cut-off factor in the magnification distribution of the form $\exp(-\mu/\mu_{\text{max}})$. As shown by Perrotta et al. (2002), for a typical brightness profile of a luminous elliptical galaxy with $r_e \simeq 5$ kpc, we expect $10 \leq \mu_{\text{max}} \leq 30$, depending on the detailed geometry of the source and of the lens and on their relative distance. The still scanty information on sizes of sub-mm galaxies (Downes et al. 1999; Ivison et al. 2001; Gear et al. 2000) suggests radii of a few kpc, implying higher maximum magnifications. On the other hand, if the SCUBA/MAMBO galaxies are really merging systems of galaxies up to 30 kpc in diameter size, then the limiting magnification will be lower. For $r_e \simeq 15$ kpc, we verified numerically that, using the same assumptions, one gets a maximum amplification between 5 (for elliptical lens potential) and 10 (for circular lens potential). Therefore, we adopted a

relatively conservative value $\mu_{\text{max}} = 10$.

Lens density profiles have been modelled as Singular Isothermal Spheres (SIS) for masses $M < 3.5 \times 10^{13} M_\odot$, and with the Navarro, Frenk & White (1997; NFW) formula for larger masses. In fact, it is found (Porciani & Madau 2000) that such a “mixed” model provides a good fit to the observed statistics of the angular splitting of QSO multiple gravitational images. However we wish to emphasize that regarding statistical magnifications SIS and NFW profiles lead to comparable results (Perrotta et al. 2002), making the present conclusions very weakly dependent on the choice of the profile.

Before moving to the results, let us consider the magnification bias on a flux-limited source sample. The integrated source counts above a flux density threshold S_ν of sources with a comoving luminosity function $\Phi(L, z)$ can be written as (e.g. De Zotti et al. 1996)

$$N(S_\nu) = \int_0^{z_0} dz \int_{L_{\text{min}}}^\infty dL \Phi(L, z) r^2(z) \frac{dr}{dz} \text{sr}^{-1}, \quad (14)$$

where r is the comoving radial distance, and

$$L_{\text{min}}(\nu) = 4\pi(1+z) r^2(z) S_\nu \frac{L(\nu)}{L[(1+z)\nu]}. \quad (15)$$

The luminosity function modified by the magnification bias reads (e.g. Pei 1995):

$$\Phi'(L, z) = \int_{\mu_{\text{min}}}^\infty d\mu \frac{p(\mu, z)}{\mu} \Phi\left(\frac{L}{\mu}, z\right). \quad (16)$$

Lensing effects on the source counts are taken into account by replacing $\Phi'(L, z)$ with $\Phi(L, z)$ in Eq. (14).

5. EFFECT OF GRAVITATIONAL LENSING ON SOURCE COUNTS

We present here our estimates for the effect of lensing on the integral number counts predicted using the model by Granato et al. (2001), at different wavelengths, focusing on the strongly lensed source fraction when all the contributing populations are taken into account; for comparison with different scenarios, we use the model by Rowan-Robinson (2001), taken as representative of successful phenomenological models. The model by Granato et al. (2001) includes three populations, namely star-forming spheroids, evolving starburst galaxies and non-evolving disc galaxies (spirals). The model by Rowan-Robinson instead includes AGNs, spirals and both high- and low-luminosity starburst galaxies. In both models, we added the contribution due to “flat”-spectrum radio sources, whose counts (kindly provided by L. Toffolatti) are based on the model by Toffolatti et al. (1998).

The contributions of different populations to the number counts at fluxes probed by SCUBA, predicted by the two models, are markedly different: while, as discussed above, according to Granato et al. (2001) SCUBA sources are mostly massive dusty spheroids at high z , in many phenomenological models there is a large tail extending to low- z , so that the mean lensing probability of sources is lower. Correspondingly, while the model by Granato et al. (2001) predicts an essentially exponential decline of the 850 μm counts with increasing flux density above a few mJy, the slope is substantially less steep in the Rowan-Robinson’s (2001) model.

This different behaviour of the counts and of the redshift distributions explains the vastly different fractions of lensed galaxies expected at bright fluxes; this difference is quantified in Figs. 8 and 9 as we describe in detail in the following. Both

figures show the integral number counts of lensed and unlensed galaxies, yielded by the two models, respectively, for the 550 (top), 850 (middle) and 1380 μm (bottom) PLANCK/HFI channels. Fig. 8 shows the unlensed, weakly lensed and strongly lensed spheroid counts, represented respectively by light dotted, heavy dashed and heavy solid lines. The heavy dotted line represents the sum over all the populations which are expected to contribute to the observed counts according to the Granato et al. (2001) model, i.e. spheroids, evolving starburst galaxies, spirals and radio sources, assuming no lensing effects. In Fig. 9 the light dotted, heavy dashed and heavy solid lines represent respectively the unlensed, weakly lensed and strongly lensed counts for the sum of AGNs, spirals and starbursts. As above, the heavy dotted line represents the sum of the contributions from all the populations plus radio sources, assuming no lensing effects. Note that for the model by Granato et al. (2001) we plotted the effect of lensing only on the forming spheroids to highlight the huge magnification bias due to the steepness of the counts, while starburst galaxies, spirals and radio sources, which are negligibly affected by lensing, are included only in the total counts, represented in Fig. 8 by the heavy dotted lines. In the case of Rowan-Robinson (2001), for all classes of sources (AGNs, spirals and starburst galaxies) the effect of lensing has been taken into account. The heavy dotted lines give the sum of weakly and strongly lensed sources, plus the contribution of radio sources, for which the effect of lensing is negligible.

It is clear from Fig. 8 that, according to the model by Granato et al. (2001) and thanks to the strong magnifications due to gravitational lensing, forming spheroids at substantial redshifts can be detected in relatively shallow surveys, such as those provided by PLANCK/HFI. The quoted 5σ detection limits for this instrument are $S_{\text{lim}} = 200, 100, 450$ mJy at 1380, 850, 550 μm , respectively. Note that, at 850 μm , this implies that the expected strongly lensed objects at fluxes larger than S_{lim} on the whole sky are $\sim 10^2$ in the Rowan Robinson (2001) scenario and $\sim 4 \cdot 10^3$ according to the model by Granato et al. (2001). Strongly lensed forming spheroids may also be detectable by forthcoming balloon experiments operating at sub-mm wavelengths, such as BLAST (Devlin et al. 2000; www.hep.upenn.edu/blast/) and ELISA (Ristorcelli et al. 2001). Such surveys may then trace the large scale distribution of the peaks of the primordial density field. The distribution of strongly lensed sources would extend to even higher fluxes in the case of magnifications larger than our conservative limit $\mu_{\text{max}} = 10$ (magnifications of up to 30 are possible according to the adopted model; cf. Perrotta et al. 2002).

A basic observable to compare the effect of strong lensing in the two scenarios is the ratio

$$\mathcal{R} = \frac{N_{\text{strong}}}{N}, \quad (17)$$

where N_{strong} represents the counts due to strongly lensed objects only, while N contains all sources from all populations without taking into account the strong lensing effect; in other words, \mathcal{R} is the ratio between the heavy-solid and the heavy-dotted lines in Figs. 8 and 9. Fig. 10 shows this ratio as a function of the 850 μm flux predicted by the two models considered above. According to the model by Granato et al. (2001), at 850 μm the ratio of strongly lensed to unlensed sources reaches the value of about 40% for fluxes slightly below 100 mJy, where the surface density of strongly lensed sources is of about 0.1 deg^{-2} . Note however that the actual fraction of strongly lensed sources may be even higher than what shown in Fig. 10. In fact we stress that, in a way which is consistent with the available observational constraints, the scenario in Fig. 8 maximizes the contributions to the counts from spiral and star-

burst galaxies; indeed the counts due to these sources at bright fluxes are significantly higher than those predicted by Rowan-Robinson (2001), as it can be seen by comparison with Fig. 9 (radio sources are the same in both models). Thus we emphasize that a large fraction of strongly lensed sources is expected at $S(850\mu\text{m}) \simeq 100$ mJy even under conservative assumptions about the dilution by unlensed populations. On the other hand, the fraction of strongly lensed sources is expected to lie below 10% for the many phenomenological models, as is the case for the model of Rowan-Robinson (2001) (see fig. 10): as we already stressed this difference is mainly due to the fact that in this scenario the SCUBA/MAMBO galaxies belong to populations which are present up to very low redshifts, being therefore negligibly affected by gravitational lensing.

It is then clear that gravitational lensing can help to discriminate among different models, all of them successfully reproducing the observed counts. Note that the strongly lensed sources detected by shallow sub-millimeter surveys, such as those carried out by PLANCK/HFI, are characterized, according to our model, by having $z > 2$ (typically, $z \simeq 3$), while most unlensed dusty (spiral and starburst) galaxies are at $z \lesssim 1$. The different populations can therefore be sifted based on the multifrequency PLANCK/HFI data thanks to their different sub-mm colours. A promising method to diagnose whether sub-mm sources are lensed has been recently proposed and discussed by Chapman et al. (2002) who estimated that the fraction of strongly lensed SCUBA sources is 3–5% at ~ 10 mJy. Although in the flux interval covered by SCUBA surveys it is difficult to discriminate among the models discussed in the present paper, the method could give interesting indications if applied to larger area surveys, i.e. to brighter fluxes (see Fig. 10).

In principle, clustered lensing galaxies can change the clustering properties of the sources in a flux-limited sample. The auto-correlation function of the lensing magnification pattern can be described as a convolution of the magnification pattern of a single lens with the correlation function of the lens centers. In our case, the magnification patterns of individual lenses have typical angular scales of at most a few arc seconds. The auto-correlation of lens centers, however, has a typical angular scale of arc minutes, and its amplitude is substantially lowered by projection because the lens population is taken from a large redshift range. Therefore, the effect of strong lensing on the clustering properties of sub-mm sources is negligible.

Weak lensing, however, can modify the autocorrelation function of a flux-limited source sample, in particular if the source counts drop as steeply with increasing flux as in the Granato et al. (2001) model. The intrinsic correlation function $w(\theta)$ of the sources then becomes $w(\theta) + (\alpha - 1)^2 w_\mu(\theta)$, where $w_\mu(\theta)$ is the magnification autocorrelation function due to weak lensing, and α is defined as $-\text{d} \ln N(> S) / \text{d} \ln S$ in the neighbourhood of the flux limit of the observation. Typical amplitudes of $w_\mu(\theta)$ for high-redshift sources are of order 0.1, and the angular scale of $w_\mu(\theta)$ is of order a few arc minutes (e.g. Bartelmann & Schneider 2001). At the same time, weak lensing will cause cross-correlations between the background sources and foreground galaxies because the latter are correlated with the weakly lensing dark-matter distribution (e.g. Dolag & Bartelmann 1997; Moessner & Jain 1998). Using this additional effect, it will be possible to disentangle the lensing-induced and the intrinsic source auto-correlations.

6. CONCLUSIONS

A major challenge for current theories of galaxy formation is to account for the evolutionary history of large spheroidal galaxies. Observations presently suggest that most of the stars (say

$> 60 - 70\%$) in large ellipticals were assembled at early epochs $z \simeq 2$ (Eales et al. 1999, Daddi et al. 2000; Cohen 2001; see Peebles 2002 for a review). On the basis of their sub-mm properties and follow-up at other wavelengths, sources detected by SCUBA and MAMBO have been associated to star-bursting proto-ellipticals (e.g. Dunlop 2001b, Scott et al. 2001).

Even the most recent semi-analytic models (Cole et al. 2000; Devriendt & Guiderdoni 2000) hinging upon the “standard” picture for structure formation in the framework of the hierarchical clustering paradigm, tuned to agree with detailed numerical simulations, are unable to account for the sub-mm counts of galaxies as well for an early ($z \simeq 2$) formation of most large ellipticals. However this may depend on choices of the values of very basic parameters, such as merging, star formation timescales, and SN feedback efficiency.

On the other hand, once a galactic halo is virialized, star formation occurs on timescales ruled by the gas cooling time and by the stellar feedback. Granato et al. (2001) pointed out that the stellar feedback (mostly supernova explosions) depresses the star formation rates of smaller haloes in a more pronounced way, yielding a star formation rate increasing with the final mass in stars M_{sph} as $SFR \simeq 100(M_{\text{sph}}/10^{11} M_{\odot})^{1.33} M_{\odot} \text{ yr}^{-1}$. The early evolution of spheroidal galaxies and of quasars growing at their centers are tightly inter-related and feed-back effects make large ellipticals form a large fraction of their stars as soon as the corresponding potential wells are in place, while the formation of stars in smaller galaxies is delayed. Therefore, according to this model, large ellipticals have large star formation rates and evolve on very small time scales (similar to those assumed in ‘monolithic’ models) and the mm/sub-mm counts are successfully reproduced. The star-formation activity, powering the dust emission, quickly declines for $z < 3$ for the most luminous (most massive) galaxies, while quasars reach their maximum luminosity. This naturally explains why very luminous quasars are more easily detected at mm/sub-mm wavelengths at redshifts larger than that ($\simeq 2.5$) of maximum quasar activity (Omont et al. 2001). As indicated by the analysis of the latter authors, a substantial fraction of the observed far-IR emission is probably powered by the starburst in the host galaxy.

In this paper statistical properties of clustering and lensing of the proto-ellipticals predicted by the model are extensively investigated and compared with recent data. Attention is focused, in particular, on two specific aspects. Since SCUBA/MAMBO galaxies are interpreted as massive galaxies at $2 \lesssim z \lesssim 6$, they are expected to be highly biased tracers of the matter distribution and therefore highly clustered. The implied angular correlation function is found to be consistent with recent results by Scott et al. (2001), Webb et al. (2002b), Peacock et al. (2000), Lagache & Puget (2000) as well as with the fluctuations in the SCUBA counts in different areas of the sky. Explicit estimates are presented for the power spectrum of temperature fluctuations due to clustering in PLANCK/HFI channels.

A second specific prediction of the model is an essentially exponential decline of the counts at $S_{850\mu\text{m}} \gtrsim 10 \text{ mJy}$ up to the fluxes at which spirals, starbursts and radio sources show up. Hints in this direction that can possibly be discerned in recent SCUBA (Scott et al. 2001; Borys et al. 2001) and MAMBO (Carilli et al. 2001) surveys are noted. As an implication of this prediction, together with the fact that sources are found at high redshifts, one has that both the gravitational lensing probability and the magnification bias on the counts are much higher than those derived for other current, phenomenological, models. We show that, according to this model, essentially all proto-spheroidal galaxies brighter than $S_{850\mu\text{m}} \gtrsim 60-70 \text{ mJy}$ are gravitationally lensed. Allowing for the other populations of sources contributing to the bright mm/sub-mm counts, we find

that the fraction of gravitationally lensed sources may be $\simeq 40\%$ at fluxes slightly below $S_{850\mu\text{m}} = 100 \text{ mJy}$. If so, large area surveys such as those to be carried out by PLANCK/HFI or by forthcoming balloon experiment like BLAST and ELISA will probe the large scale distribution of the peaks of the primordial density field. The multifrequency observations provided by PLANCK will help in discriminating between high redshift sources (with high lensing probability), relatively nearby starburst and spiral galaxies, and radio sources.

ACKNOWLEDGMENTS

We are grateful to P. Panuzzo and L. Toffolatti for help with the counts of spheroidal galaxies and radio sources, respectively. This work was supported in part by ASI, MURST and UE.

REFERENCES

- Almaini O. et al., 2002, astro-ph/0108400
 Archibald E.N., Dunlop J.S., Jimenez R., Friaa A.C.S., McLure R.J., Hughes D.H., 2001, ApJ, submitted, astro-ph/0108122
 Barger A.J., Cowie L.L., Sanders D.B., Fulton E., Taniguchi Y., Sato Y., Kawara K., Okuda H., 1998, Nat 394, 248
 Barger A.J., Cowie L.L., Sanders D.B., 1999a, ApJ 518, L5
 Barger A.J., Cowie L.L., Trentham N., Fulton E., Hu E.M., Songaila A., Hall D., 1999b, AJ 117, 102
 Bartelmann M., Schneider P., 2001, Phys. Rep. 340, 291
 Baugh C.M., Cole S., Frenk C.S., Lacey C.G., 1998, ApJ 498, 504
 Baugh C.M., Benson A.J., Cole S., Frenk C.S., Lacey C.G., 1999, MNRAS, 305, 21
 Benitez N., Broadhurst T.J., Bouwens R.J., Silk J., Rosati P., 1999, ApJ 515, L65
 Bertoldi F., Carilli C.L., Menten K. M., et al., 2000, A&A 360, 92
 Bertoldi F., Menten K.M., Kreysa E., Carilli C.L., Owen F., 2001, astro-ph/0010553
 Blain A. W., 1996, MNRAS, 283, 1340
 Blain A. W., 1997, MNRAS 290, 553
 Blain A.W., 1998a, MNRAS 295, 92
 Blain A.W., 1998b, MNRAS 297, 511
 Blain A.W., 1999, MNRAS 304, 669
 Blain A.W., 2000, in Cosmological Physics with Gravitational Lensing, Kneib J.-P., Mellier Y., Moniez M., Tran Thanh Van J. eds., Rencontres de Moriond XX, ed. Frontières, Gif sur Yvette, astro-ph/0007196
 Blain A.W., Ivison R.J., Kneib J.-P., Smail I., 2000, in ‘The Hy-Redshift Universe: galaxy formation and evolution at high redshift’, eds. A. J. Bunker & W. J. M. van Breughel, ASP Conf. Ser. 193, p. 246
 Blain A. W., Longair M. S., 1993, MNRAS 264, 509
 Blain A.W., Smail I., Ivison R.J., Kneib J.-P., 1999, MNRAS 302, 632
 Blanton M., Cen R., Ostriker J.P., Strauss M.A., 1999, ApJ 522, 590
 Borys C., Chapman S., Halpern M., Scott D., 2001, astro-ph/0107515
 Broadhurst T.J., Bowens R.J., 2000, ApJ 530, 53
 Carilli C.L., Bertoldi F., Bertarini A., Menten K.M., Kreysa E., Zylka R., Owen F., Yun M., 2001, in Deep Millimeter Surveys: Implications for Galaxy Formation, eds. J. Lowenthal & D.K. Hughes, World Scientific
 Cavaliere A., Vittorini V., 1998, in *The Young Universe: Galaxy Formation and Evolution at Intermediate and High Redshift*, S. D’Odorico, A. Fontana & E. Giallongo eds., ASP conf. ser. 146, p. 26
 Chapman S.C., Smail I., Ivison R.J., Blain A.W., 2002, astro-ph/0204086
 Cohen J.G., 2001, AJ 121, 2895
 Cole S., Lacey C.G., Baugh C.M., Carlton M., Frenk C.S., 2000, MNRAS 319, 168
 Daddi E., Cimatti A., Renzini A., 2000, A&A 362, L45
 Dekel, A., & Lahav, O., 1999, ApJ 520, 24
 Devlin M.J. and the BLAST collaboration, 2000, astro-ph/0012327
 Devriendt J.E.G., Guiderdoni B., 2000, A&A 363, 851
 De Zotti G., Franceschini A., Toffolatti L., Mazzei P., Danese L., 1996, Ap. Lett.Comm., 35, 289
 Dolag, K., Bartelmann, M., 1997, MNRAS, 291, 446
 Dole H., Gispert R., Lagache G., et al., 2001, A&A 372, 364
 Downes D. et al., 1999, A&A 347, 809
 Dunlop J.S., 2001a, New Astronomy Review, 45, 609
 Dunlop J.S., 2001b, in Deep Millimeter Surveys: Implications for Galaxy Formation, eds. J. Lowenthal & D.K. Hughes, World Scientific
 Dwek E., Arendt R.G., Hauser M.G., et al., 1998, ApJ 508, 106
 Eales S., Lilly S., Gear W., Dunne L., Bond J.R., Hammer F., Le Fèvre O., Crampton D., 1999, ApJ 515, 518
 Eales S., Lilly S., Webb T., Dunne L., Gear W., Clements D.L., Yun M., 2000, AJ, 120, 2244
 Elbaz D., Cesarsky C. J., Fadda D., et al., 1999, A&A 351, L37
 Finkbeiner D.P., Davis M., Schlegel D.J., 1999, ApJ 524, 867
 Fixsen D.J., Dwek E., Mather J.C., Bennett C.L., Shafer R.A., 1998, ApJ 508, 123

- Fox M.J., Efstathiou A., Rowan-Robinson M., et al., 2001, MNRAS, accepted, astro-ph/0107585
- Franceschini A., Aussel H., Cesarsky C.J., Elbaz D., Fadda D., 2001, A&A, submitted, astro-ph/0108292
- Franceschini A., De Zotti G., Toffolatti L., Mazzei P., Danese L., 1991, A&AS 89, 285
- Franceschini A., Silva L., Fasano G., Granato G.L., Bressan A., Arnouts S., Danese L., 1998, ApJ 506, 600
- Franceschini A., Mazzei P., De Zotti G., Danese L., 1994, ApJ 427, 140
- Fry J.N., 1996, ApJ, 461, L65
- Gear W.K., Lilly S.J., Stevens J.A., Clements D.L., Webb T.M., Eales S.A., Dunne L., 2000, MNRAS 316, L51
- Giavalisco M., Dickinson M., 2001, ApJ 550, 177
- Giavalisco M., Steidel C.C., Adelberger K.L., Dickinson M.E., Pettini M., Kellogg M., 1998, ApJ, 503, 543
- Granato G.L., Lacey C.G., Silva L., Bressan A., Baugh C.M., Cole S., Frenk C.S., 2000, ApJ 542, 710
- Granato G.L., Silva L., Monaco P., Panuzzo P., Salucci P., De Zotti G., Danese L., 2001, MNRAS 324, 757
- Guiderdoni B., Bouchet F.R., Puget J.L., Lagache G., Hivon E., 1997, Nat 390, 257
- Guiderdoni B., Hivon E., Bouchet F.R., Maffei B., 1998, MNRAS 295, 877
- Haehnelt M.G., Rees M.J., 1993, MNRAS 263, 168
- Haehnelt M.G., Natarajan P., Rees M.J., 1998, MNRAS 300, 817
- Haiman Z., Knox L., 2000, ApJ, 530, 124
- Hauser M. G., Arendt R. G., Kelsall T., et al., 1998, ApJ 508, 25
- Hughes D.H., Serjeant S., Dunlop J., et al., 1998, Nat 394, 241
- Iverson R.J., Smail I., Frayer D. T., Kneib J.-P., Blain A.W., 2001, ApJ 561, L45
- Jing Y.P., 1998, ApJ, 503, L9
- Kauffmann G., 1996, MNRAS 281, 487
- Kauffmann G., Charlot S., White S.D.M., 1996, MNRAS 283, 117
- Lacey C., Cole S., 1993, MNRAS, 262, 649
- Lagache G., Abergel A., Boulanger F., Désert F.X., Puget J.-L., 1999, A&A 344, 322
- Lagache G., Haffner L.M., Reynolds R.J., Tuft S.L., 2000, A&A 354, 247
- Lagache G., Puget J.L., 2000, A&A, 355, 17
- Loveday J., Tresse L. & Maddox S.J., 1999, MNRAS, 310, 281
- Magliocchetti M., Maddox S.J., Lahav O., Wall J.V., 1999, MNRAS, 309, 943
- Magliocchetti M., Bagla J., Maddox S.J., Lahav O. 2000, MNRAS 314, 546
- Magliocchetti M., Moscardini L., Panuzzo P., Granato G.L., De Zotti G., Danese L. 2001a, MNRAS, 325, 1553
- Magliocchetti M., Moscardini L., De Zotti G., Granato G.L., Danese L., 2001b, proceedings of the conference "Where's the Matter? Tracing Dark and Bright Matter with the New Generation of Large Scale Surveys", June 2001, Treyer & Tresse Eds, Frontier Group, astro-ph/0107597
- Marinoni C., Hudson M.J., 2001, ApJ, submitted (astro-ph/0109134)
- McKay T.A., Sheldon E.S., Racusin J., et al., 2001, ApJ, submitted, astro-ph/0108013
- Moscardini L., Coles P., Lucchin F., Matarrese S., 1998, MNRAS, 299, 95
- Menanteau F., Ellis R.S., Abraham R.G., Barger A.J., Cowie L.L., 1999, MNRAS 309, 208
- Moessner, R., Jain, B., 1998, MNRAS, 294, L18
- Narayanan V.K., Berlind A.A., Weinberg D.H., 2000, ApJ 528, 1
- Navarro J.F., Frenk C.S., White S.D.M., 1997, ApJ 490, 493
- Omont A., Cox P., Bertoldi F., McMahon R.G., Carilli C., Isaak K.G., 2001, A&A 374, 371
- Peacock J. A., 1982, MNRAS 199, 987
- Peacock J.A., 1997, Cosmological Physics, Cambridge University Press
- Peacock J.A., Dodds S.J., 1996, MNRAS, 267, 1020
- Peacock J.A., Rowan-Robinson M., Blain A.W., et al., 2000, MNRAS 318, 535
- Pearson C.P., Matsuhara H., Onaka T., Watarai H., Matsumoto T., 2001, MNRAS 324, 999
- Pearson C.P., Rowan-Robinson M., 1996, MNRAS 283, 174
- Peebles P.J.E., 1980, The Large-Scale Structure of the Universe, Princeton University Press
- Peebles P.J.E., 2002, in "A New Era in Cosmology", ASP Conf. Ser., N. Metcalfe & T. Shanks eds., in press, astro-ph/0201015
- Pei Y.C., 1995, ApJ 440, 485
- Perrotta F., Baccigalupi C., Bartelmann M., De Zotti G., Granato G.L., 2002, MNRAS 329, 445
- Pettini M., Shapley A. E., Steidel C. C., Cuby J., Dickinson M., Moorwood A. F. M., Adelberger K. L., Giavalisco M., 2001, ApJ 554, 981
- Porciani C., Madau P., 2000, ApJ 532, 679
- Press W.H., Schechter P., 1974, ApJ, 187, 425
- Puget J.-L., Abergel A., Bernard J.-P., Boulanger F., Burton W.B., Desert F.-X., Hartmann D., 1996, A&A 308, L5
- Ristorcelli I., Bernard J.-P., Stepnik B., et al., 2001, The Promise of the Herschel Space Observatory. Eds. G.L. Pilbratt, J. Cernicharo, A.M. Heras, T. Prusti, & R. Harris. ESA-SP 460, p. 301
- Roche N., Eales S.A., 1999, MNRAS 307, 703
- Rodighiero G., Franceschini A., Fasano G., 2001, MNRAS 324, 491
- Rowan-Robinson M., 2001, ApJ 549, 745
- Saunders W., Rowan-Robinson M., Lawrence A., Efstathiou G., Kaiser N., Ellis R.S., Frenk C.S., 1990, MNRAS 242, 318
- Schlegel D.J., Finkbeiner D.P., Davis M., 1998, ApJ 500, 525
- Scodreggio M., Silva D., 2000, A&A 359, 953
- Scott D., White M., 1999, A&A 346, 1
- Scott S.E., Fox, M.J., Dunlop J.S., et al., 2001, MNRAS, submitted, astro-ph/0107446
- Seljak U., Zaldarriaga M., 1996, ApJ, 469, 437.
- Sheth R. K., Tormen G., 1999, MNRAS, 308, 119
- Silk J., Rees M.J., 1998, A&A 331, L1
- Silva L., Granato G.L., Bressan A., Danese L., 1998, ApJ 509, 103
- Smail I., Ivison R.J., Blain A.W., 1997, ApJ 490, L5
- Smail I., Ivison R.J., Owen F.N., Blain A.W., Kneib J.-P., 2000, ApJ 528, 612
- Smail I., Ivison R.J., Blain A.W., Kneib J.-P., 2001, in Deep Millimeter Surveys: Implications for Galaxy Formation, eds. J. Lowenthal & D.K. Hughes, World Scientific
- Smail I., Ivison R.J., Blain A.W., Kneib J.-P., 2002, MNRAS 331, 495
- Takeuchi T.T., Kawabe R., Kohno K., Nakanishi K., Ishii T.T., Hirashita H., Yoshikawa K., 2001, PASP 113, 586
- Toffolatti L., Argueso Gomez F., De Zotti G., Mazzei P., Franceschini A., Danese L., Burigana C., 1998, MNRAS, 297, 117
- Totani T., Yoshii J., 1997, ApJ 501, L177
- Treu T., Stiavelli M., 1999, ApJ 524, L27
- Turner E.L., Ostriker J.P., Gott J.R., 1984, ApJ 284, 1
- Webb T.M., Eales S., Foucaud S., et al., 2002a, ApJ, submitted, astro-ph/0201181
- Webb T.M., Eales S., Lilly S.J., et al., 2002b, ApJ, submitted, astro-ph/0201180
- Zepf S.E., 1997, Nat 390, 377